Reactivity of coke in relation to sulfur level and microstructure

Gøril Jahrsengene, Arne Petter Ratvik, Stein Rørvik, Lorentz Petter Lossius, Richard G. Haverkamp, Ann Mari Svensson

Abstract

The quality of coke materials available for anodes for the aluminium industry is changing and industrial cokes with higher impurity levels are now introduced. The cokes in the anodes must meet specifications with respect to impurity levels to ensure proper operation in the electrolysis cells, and a desired quality of the aluminium metal. The presence of sulfur has been observed to reduce the CO_2 reactivity and a certain level of sulfur is therefore targeted in the anodes. In this work, the significance of varying sulfur and metal impurity content in industrial cokes were evaluated with respect to CO_2 reactivity, accessible surface area, pore size distribution, surface oxide groups and crystallite reactive edge planes. While relatively similar cokes are observed to give a lower reactivity with increasing sulfur content, cokes that have distinct differences in surface properties can have dissimilar reactivity despite identical sulfur content. Correlations between pore size distribution and presence of S-S bound sulfur, possibly condensed S_x, was also observed.

Keywords: Petroleum coke, Sulfur, CO_2 reactivity,

Introduction

In electrolytic production of aluminium, carbon is oxidized to CO_2 during the reduction of alumina (Al_2O_3). Prebaked anodes made of calcined petroleum coke, coal tar pitch and recycled anode butts provide the carbon for the reaction. The theoretical amount of carbon is 0.33 kg to produce 1 kg of Al, while in practice it is higher. This is caused by the back reaction, where produced Al is oxidized by CO_2 forming Al_2O_3 and CO. The anode may also react with CO_2 or air. The air reactivity can be reduced by limiting the exposure to air by good covering of the anodes, which is well incorporated in modern cells. The reaction between produced CO_2 and carbon is assumed to be affected by the presence of sulfur level in the anodes.

The changes in the quality of the petroleum coke will affect the performance of the anode in the pot room. In addition to the less dense coke materials produced by the refining industry, the cokes also have an increasing amount of sulfur and other metal impurities compared to previously used cokes [1, 2]. An anode with more open porosity will be more susceptible to air and CO_2 reactivity, and many of the metals catalyse these reactions. A good overview of the effect of impurities can be found elsewhere [3]. Beside the possible increase in reactivity due to metals present in the coke, most metals end up in the finished aluminium product. Thus, the metal specifications for vanadium, nickel, iron and silicon in the anodes is usually decided by the tolerance level of these in the primary aluminium rather than the increase in carbon oxidation. Sulfur is believed to have a positive effect on the carboxy reactivity, as high sulfur anodes has been shown to have a lower reactivity. The inhibiting effect caused by more sulfur comes at the expense of more SO_2 produced, and for plants without SO_2 scrubbing the sulfur content may be limited by SO_2 emission permission.

Sulfur and its effect on reactivity has been subject to many investigations, and it is assumed that the positive effect sulfur has on the CO_2 reactivity comes in combination with the metal impurities, as the effect of sulfur alone is possibly negative for both air and CO_2 reactivity when evaluating sulfur without other impurity interference [4]. The observed positive effect may be caused by the formation of inactive metal-sulfur complexes during carbonization [5, 6], however, most of the conclusions are based on adding impurity elements in the production of anodes. This will not necessary represent industrially produced anodes, as doped anodes may not have the same chemical state properly incorporated within the coke structure, which may give misleading results compared to the industrial cokes.

Sulfur speciation of selected cokes was previously performed by the authors by the X-ray absorption near-edge structure (XANES) technique [7]. Five cokes were investigated, which varied significantly with respect to content of sulfur (1.4 to 5.5 wt%) and content of metal impurities. Furthermore, there was a poor correlation between the sulfur content and CO_2 reactivity of some of these cokes. The ratio between S-S bound sulfur (which can result from elemental sulfur, pyritic sulfur and R-S-S-R sulfur) and other aromatically bound sulfur (e.g. thiophenes) varied significantly. The amount of S-S bound sulfur was found to inversely correlate with the CO_2 reactivity.

The aim of this work has been to gain an improved understanding of a wider range of factors that might affect the CO_2 reactivity of the cokes, like variations in reactive surface area of cokes of similar particle size, as well as variations in surface structure (i.e. ratio of edge to basal planes) or surface chemistry. Reactive surface area was estimated based on Hg intrusion porosimetry and N_2 adsorption experiments. The latter was also used for analysis of surface structure (ratio of edge, basal and defect sites). Possible differences in surface chemistry were also studied by monitoring the release of CO_2 and CO during heating.

Materials and Method

Previously reported data and properties [7] of the five industrial cokes are summarized in Table 1. Impurity content (sulfur and metals) was measured by X-Ray Fluorescence (XRF), the optical texture evaluated by mosaic and fiber index found by light microscopy, and CO_2 reactivity reported as mass loss during a standard mass loss test (ISO-12981-1 Standard RDC-1141). The S-S bound sulfur found by XANES is reported as fraction of total sulfur content and wt%.

Table 1. Composition the five cokes. "Total metals" include V, Fe, Ni, Na, Mg, Al, Si and Ca.

	S (wt%)	**S-S bound sulfur (fraction/wt%)**	**CO_2 reactivity (% mass loss)**	**Total metals (ppm)**	**Optical structure**
Coke A	1.42	0.16 / 0.23	7.5	761	Anisotropic
Coke B	3.56	0.20 / 0.71	6.0	1323	Anisotropic
Coke C	5.54	0.21 / 1.18	4.2	1356	Anisotropic
Coke D	3.86	0.41 / 1.56	3.6	1668	Anisotropic
Coke E	4.42	0.53 / 2.34	4.0	2009	Isotropic

The same cokes were investigated for varying surface properties. An evaluation of the pore size distributions was done by two parallels of Hg intrusion porosimetry using AutoPore IV 9520 (from Micromeritics) on 1-2 mm coke particles (ASTM D4404-10). Hg is forced into pores where the force/pressure used will be equivalent to a pore size, and the intrusion volume is measured and the Washburn equation is used to generate volume and size distributions (cylindrical pores are assumed) [8].

Nitrogen adsorption at -198.5°C was performed on the full relative pressure range (up to $P/P_0 = 0.98$) on crushed coke particles <25 μm from the 1-2 mm fraction using a 3Flex 3500 Chemisorption Analyser (Micromeritics). Graphite powder (SLP30 from IMERYS) was used as a reference. The samples were degassed at 300 °C for 10 hours before analysis. Specific surface area was determined by the Brunauer-Emmett-Teller (BET) theory [9]. In addition the Barret-Joyner-Halenda (BJH) pore size distribution [10] were extracted from the software of the instrument. The adsorption data was used to find the relative contribution of edge:basal:defect sites based on a model established by Olivier [11] using

density functional theory (DFT). Different adsorption potentials, expressed in kelvin (K), are used to account for the heterogeneity of the surface. For graphitic materials it is assumed that prismatic/edge sites are in the 20-49 K range, basal planes in the 50-60 K range, and higher energy regions of 61-100 K for defects [12]. Surface defects can be small, slit-like pores (<1 nm diameter), surface steps as well as attributed to surface groups. Two or three parallels were done on freshly crushed samples.

Surface oxides, assumed to be attached to edge sites, will decompose to CO and CO_2 during heat treatment. A rapid temperature ramping program with an analyser (ONH386 Series) from LECO was used. The CO and CO_2 is first detected by separate IR cells, to see what gases goes off when (and indirectly at which temperatures), while the total oxygen is found after the gas pass through heated copper oxide to convert CO to CO_2 and then to a separate IR detector. By comparing to graphite, oxygen assumed to be related to metal impurities, can be excluded from the surface oxides. Samples of 0.1 g crushed coke particles (particle size <25 µm) from the 1-2 mm fraction were packed in tin capsules and the measurements were done by ramping of power linearly in the temperature range from 500 to 3000 °C within 600 s. Two parallels of each coke and one from graphite powder were obtained.

The data obtained from nitrogen adsorption and desorption, Hg porosimetry and LECO oxygen analysis were combined and evaluated together with the previously obtained data presented in Table 1.

Results and Discussion

Hg intrusion porosimetry

The (smoothed) pore size distribution in the cokes (1-2 mm fraction) found by Hg intrusion is presented in Fig. 1. The measurements above 60 µm are excluded in the analysis of intrusion volume, surface area and average pore size in Table 2 as it is likely a result of intrusion between grains, while data below 0.1 µm is assumed affected by destruction of the grains at high pressures and is also excluded.

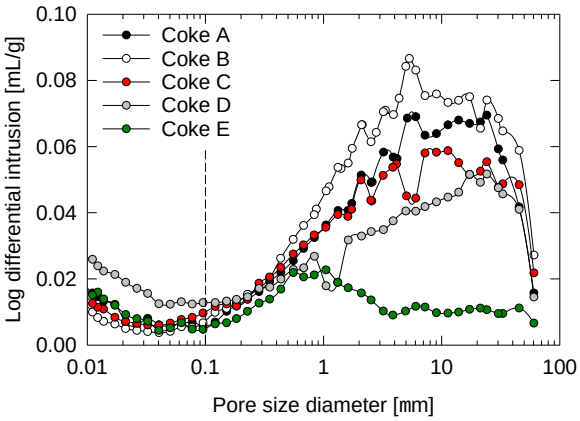

Fig. 1. Pore size distribution as a function of intrusion volume.

There are significant differences between the cokes. Coke E has the lowest intrusion volume and a centre around 1 µm, resulting in a low total surface area. Coke D has a wider distribution and lower intrusion volumes than cokes A-C, resulting in low surface area compared to the other anisotropic cokes. Considering the region of pore diameters from 0.1 to 60 µm the average pore size is decreasing steadily from A to E (Table 2) while the total pore area is highest for coke B.

Table 2. The measured intrusion volume, estimated pore diameter and area for pores above 0.1 µm and below 60 µm, reference to Fig. 1. Average of two measurements, with standard deviation largest for cokes B and E.

	Intrusion volume [mL/g]	**Area [m^2/g]**	**Average pore diameter (d=4V/A) [nm]**
Coke A	0.1222	0.268	1826
Coke B	0.1363	0.311	1751
Coke C	0.1091	0.289	1508
Coke D	0.0899	0.257	1388
Coke E	0.0039	0.174	895

The high increase in measured intrusion volume at high pressures, observed to be increasing nearing 0.01 µm in Fig. 1 (and in fact increasing a lot in the range not presented), can be assumed to be affected by failure of the coke microstructure; at 10 nm the pressure is equivalent to 1.4 tons/cm^2. The method is insufficient at these pressures because the result reflects the integrity of the grains rather than the porosity. To investigate micro- and mesoporosity in cokes, Hg intrusion porosimetry is clearly not the best option. This range needs to be evaluated further with other methods, for example pore size distributions obtained by N_2 adsorption.

Nitrogen adsorption

Nitrogen adsorption and desorption isotherms are shown in Fig. 2a for a selection of the cokes and the graphite. The isotherms resemble the type II isotherms defined by IUPAC [13], usually observed for non-porous and macroporous materials. The change to the linear middle section corresponds to the change from monolayer to multilayer adsorption, and the graphs increase without limit close to P/P_0=1. There is a small hysteresis observed and the sharp step-down of the desorption branch is observed approximately at P/P_0~0.4-0.5. This is defined as a H4 hysteresis loop, often observed for carbons with pore structures including several different pore sizes in the network (micro- mesoporous carbons). H4 can also be related to slit-shaped pores and microporosity. This behaviour is expected for petroleum cokes. All the cokes and the graphite have this hysteresis, but for coke E the relative difference between adsorption and desorption in the linear hysteresis area was larger than the other cokes. Cokes B and C had the smallest hysteresis.

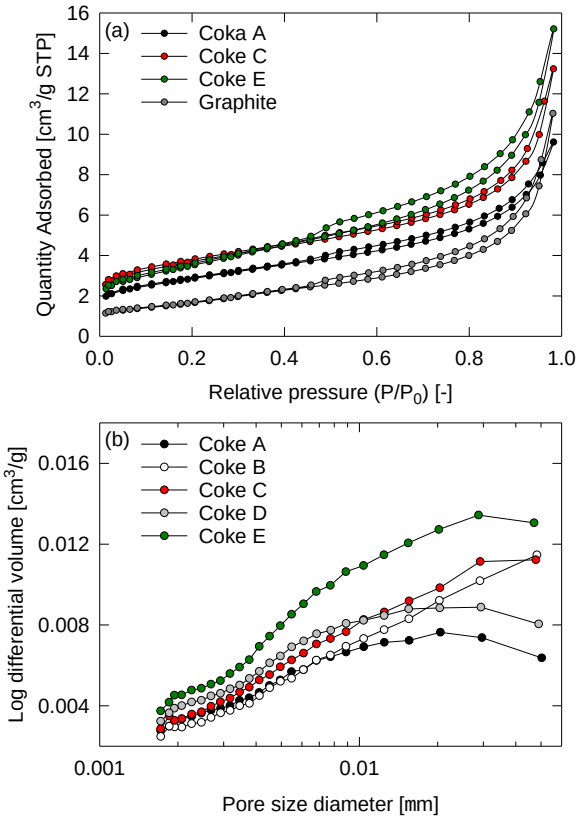

Fig. 2. (a) Isotherms for cokes A, C, E and graphite, showing the quantity of N_2 adsorbed at varying relative pressures (P/P_0), (b) BJH pore size distribution.

The BJH adsorption pore size distribution in the mesopore area, with pore sizes between 2 nm and 50 nm, is presented in Fig. 2b. According to the results, coke A has the least amount of small pores, and coke E has more small pores than the other cokes. At the lowest pore size range, cokes A, B and C are quite similar, but variations are observed from ~4 nm. N_2 adsorption is a non-destructive method, and the behaviour of the cokes of pore sizes below 0.1 µm do not reflect the observations from mercury intrusion, which was clearly affected by cracking of grains at high pressures. The isotropic coke is presented in Fig. 2b to have more pores in the entire range below 0.1 µm than the other cokes, which confirm this theory. The BJH method use the Kelvin equation in combination with the t-curve (carbon black defined solid) and are known to under-estimate contribution from narrow mesopores, indicating that the method is not suited for determining specific differences for pore sizes below 5-10 nm.

The complete picture of the porosity of the cokes are still not established combining Hg porosimetry and N_2 adsorption. It can be argued that Hg porosimetry gives good and comparable data above 0.1 µm as significant differences between cokes are observed, while the isotropic coke E has a significantly smaller average pore size than the rest of the cokes. N_2 adsorption also shows this coke has a larger contribution of pores down to 0.01 µm. A better analysis of the even smaller pores may be investigated using molecular simulations or DFT given a good model system supported by sufficient experimental data, but is not done in this study.

The surface coverage of edge, basal and defect area were determined by nitrogen adsorption and DFT modelling in the software. A typical plot of the distribution of incremental surface area vs. energy is presented for graphite in Fig. 3a, where both the typical edge site energy (42 K) and basal plane energy (58 K) can be observed. The summarized result of the areas assumed to be edge, basal and defect sites for graphite and cokes are presented in Fig. 3b. All cokes have a high portion of edge sites compared to graphite. For cokes A to C the portion of edge sites are increasing with increasing sulfur content

(which increase from A to C), while cokes D and E have a significantly lower portion of edge sites. Both defect sites and edge planes indicate insufficiencies in the carbon material and less ordered structure. Coke D and E appear to have more of the non-reactive basal planes.

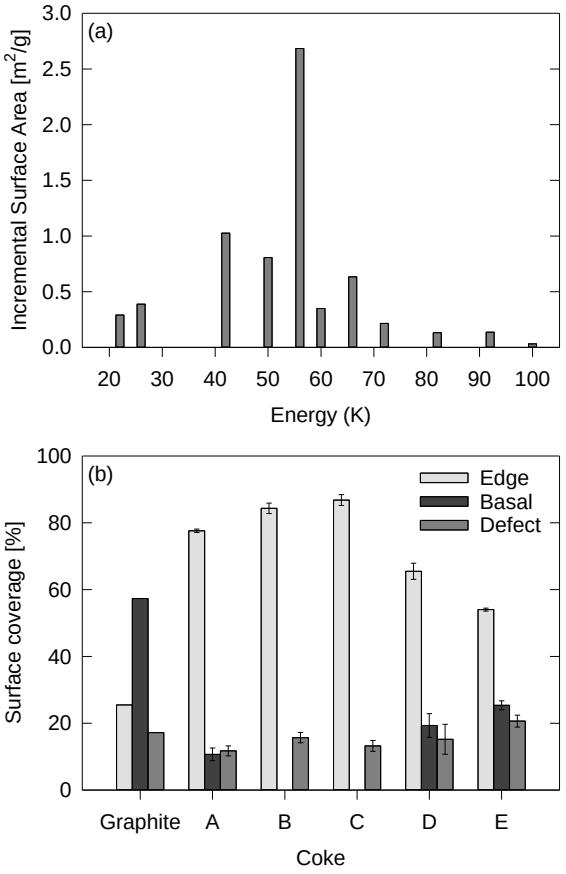

Fig. 3. (a) Typical plot of incremental surface area vs. energy for graphite, and (b) edge site, basal planes and defect sites surface coverage of graphite and industrial cokes A-E. Error bars for the cokes show one standard deviation where n=3 for cokes A-D and n=2 for coke E.

Surface and metal oxides

Information about the content of oxides in the cokes, obtained by combustion coke to CO and CO_2 measured by a LECO oxygen analyser, is presented in Fig. 4 and Table 3. The total amount of oxygen varies from 0.128 wt% in coke A, to 1.07 wt% in coke C. Comparing release of CO_2 for graphite and cokes in Fig. 4a it is clear that all but coke A have one or several additional peaks above 1450 °C. A similar limit is found in the release of CO in Fig. 4b. By separately integrating the CO_2 and CO graphs, one can find the oxygen related to surface oxide groups assumed to be present below 1450 °C, and oxide related to metal oxides as the higher temperature peaks. Release of CO_2 from coke is an indication of carboxylic, anhydride and lactone groups, while phenol, carbonyl, anhydride, ether and quinone groups give rise to CO gas [14]. Below 1450 °C both CO_2 and CO peaks appear to be similar but with different intensities (the intensity do not reflect the actual amount of oxygen). Based on these results, no significant differences in the surface chemistry of the cokes could be detected, although the ramping of power (temperature) is far too high for detection of specific surface compounds. The technique is mostly used to find the total amount of oxygen in materials.

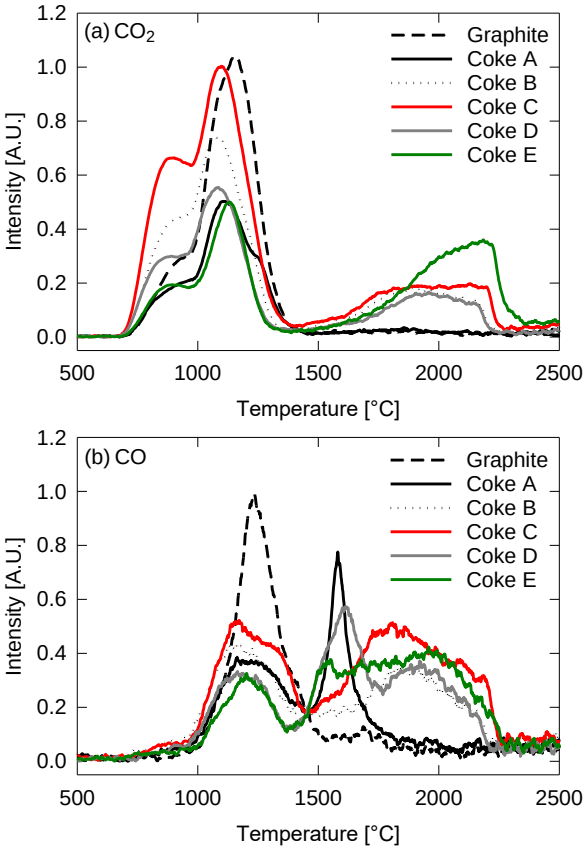

Fig. 4. Evolved (a) CO_2 and (b) CO from combusted oxides in cokes and graphite.

Table 3. The oxygen content in the cokes. The evaluation of surface oxides originates from data obtained below 1450 °C.

	Total oxygen (wt%)	**Oxygen as CO_2 (wt%)**	**Oxygen as CO (wt%)**	**CO:CO_2 for surface groups**
Graphite	0.132	0.057	0.075	1.1
Coke A	0.128	0.040	0.088	1.2
Coke B	0.578	0.060	0.518	5.1
Coke C	1.07	0.081	0.989	6.2
Coke D	0.652	0.053	0.599	5.3
Coke E	0.877	0.074	0.803	2.9

Cokes B, C and D all have more than 5 times more CO than CO_2 and coke E has 3 times as much. This indicates that phenol, carbonyl, anhydride, ether and quinone surface groups are dominating in the cokes. The similar content of CO and CO_2 for coke A indicates that perhaps the limit of 1450 °C is not sufficient for the CO graph, as coke A, with little metal oxides, have a significant peak in the 1500 to 1700 °C range. This was attributed to metal oxides as the graphite had no response in this range, but this peak may indicate differently. As cokes D and E also have peaks in this area the CO:CO_2 ratio will increase for these cokes as well as for coke A if this is accounted for, and cokes D and E will in fact have some additional oxide groups that may affect the reactivity. For all cokes but the isotropic coke E there are more surface oxygen than metal oxygen.

Evaluations of CO_2 reactivity

The CO_2 reactivity will depend on the surface area accessible for the reaction between CO_2 and C, where diffusion of the CO_2 into the pores is of high importance. Although the small pores contribute to a larger surface area, transport of CO_2 gas is limited, and the pore walls are thus not accessible for the reaction to a significant extent. In large pores, the mass transport can be described by the conventional binary diffusion coefficient, but when the pore size approach the mean free path of the CO_2 molecules, the slow Knudsen diffusion quickly starts to dominate [15]. The test was done on at 1000 °C and 0.2 MPa, where the mean free path (λ) for CO_2 is 365 nm. Knudsen diffusion is said to be dominant when $K_n>10$ and negligible when $K_n<0.1$, where the so-called Knudsen number is defined as $K_n=\lambda/d_p$, where d_p is the pore diameter. This means that pores below approximately 40 nm does not contribute to the reactive area as the total diffusion here is very low. The total diffusion constant is a function of both the (constant) mass diffusion constant D_{ab}, approximately 1.1 cm^2/s for a CO_2-CO binary system at the given conditions using the Slattery-Bird correlation [16], and Knudsen diffusion constant D_K, proportional to d_p, by

$$\frac{1}{D_{tot}} = \frac{1}{D_{ab}} + \frac{1}{D_K}$$

Assuming pore diameters larger than 0.1 µm (i.e. corresponding to the region where we have reliable Hg intrusion data), D_{tot} decrease with more than 80 % compared to a situation where D_{ab} dominates (i.e. no or large pores). The calculated surface area, excluding pore sizes <0.1 µm, was used to normalize the CO_2 reactivity data in Fig. 5, however, moving the included range to higher pore sizes do not result in a significant difference in the observed trends. All but coke E have a relatively similar pore size distribution above 0.1 um, and thus the reactivity of coke E is the only one that will change notably compared to cokes A to D. Fig. 5 shows the reactivity with respect to total sulfur content, S-S bound sulfur and organic sulfur, and cokes A, D and E is also normalized to subtract the coverage of basal planes found by DFT (no basal planes were found for B and C).

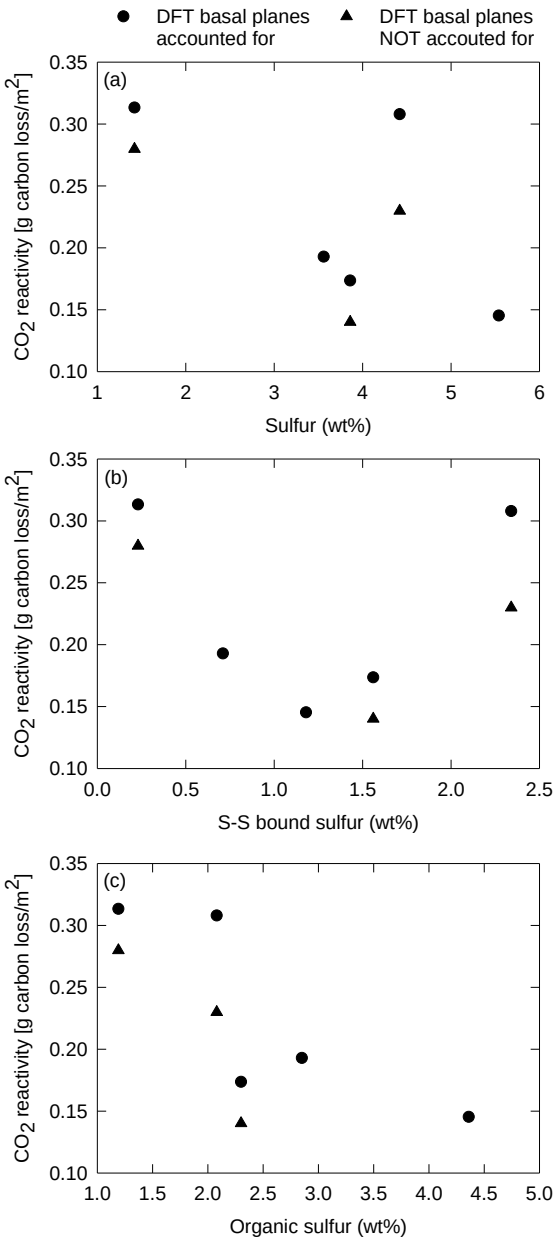

Fig. 5. The normalized reactivity, with area corresponding to pore size >0.1 µm and possible subtraction of basal planes, plotted with respect to (a) total sulfur, (b) S-S bound sulfur and (c) organic sulfur. Note that the y-value of each coke is identical in all figures, only the sulfur amounts vary (Table 1).

Based on Fig. 5, the differences originally observed in mass loss during the reactivity test is likely due to differences in the available area for the reaction to occur. With the exception of coke E, decreasing reactivity with more sulfur, S-S bound sulfur and organic sulfur was observed. Comparing Fig. 5a to 5c, it appears that the correlation of lower reactivity and S-S bound sulfur previously observed may be indirect. Fig. 6 show that the amount of S-S bound sulfur follow the area for pores <50 nm (found by BJH adsorption data), which may also explain the presence of S-S bound sulfur, as many compounds containing S-S bonds (elemental sulfur for example), is not expected to be stable at the typical calcination temperatures. If S-S bound sulfur is present in the smaller pores, and these are not accessible for the CO_2 reaction, the S-S bound will not contribute to the inhibiting reaction. The proper chemistry of this S-S compound is still unknown, but S_x (x=2,4,6 and 8), formed from organic sulfur in pores,

trapped in small pores during heat treatment and subsequently condensed, have previously been discussed as an option [4].

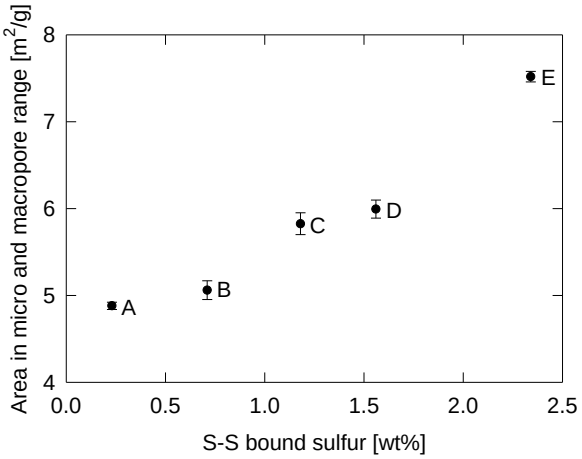

Fig. 6. The relationship between area in the BJH evaluations (2-50 nm) and the S-S bound sulfur.

Regarding the cokes A, B and C, these cokes have similar surface areas and pore size distribution, the N_2 adsorption isotherms are similar and the DFT analysis gave almost complete surface coverage of reactive sites. The largest observed difference was coke A on the BJH pore size distribution and the oxygen surface groups. The intermediate step of CO_{ads} formation in the Bodouard reaction may also be affected by the differences in the oxygen surface groups between the cokes. Although similar below 1450 °C, cokes D and E had an additional peak in the 1500-1700 °C range that may be related to surface oxides, and thus affect the reaction. Coke D and E were also shown to have a different pore size distribution explaining the low reactivity, as narrow pores are inaccessible for the reacting gases compared to the outer surface area/wide pores. A higher portion of the non-reactive basal planes was also observed in these cokes. The sulfur content, in practice the organic sulfur content, seems to be correlated to the lowering of reactivity in high-sulfur cokes, as S-S bound sulfur, possibly condensed S_x, is most likely trapped in narrow pores.

Conclusions

Selected cokes were investigated with respect to porosity, pore size distribution, surface chemistry and surface structure, and the investigations gave a better insight in different factors affecting CO_2 reactivity in cokes. Poor correlations between the reactivity and the amount of sulfur present in the cokes could be explained by the accessible surface area. The isotropic coke also has a much lower average pore size and a large amount of pores in the micro and macroporous range than the rest of the cokes, which can result in low structural integrity of the grains. Higher amount of S-S bound sulfur is observed in the cokes with smaller average pore size, indicating that any correlating relationship between S-S bound sulfur and CO_2 reactivity might be indirect.

Acknowledgements

Financial support from the Norwegian Research Council and the partners Hydro Aluminium, Alcoa, Elkem Carbon and Skamol through the project ”Reactivity of Carbon and Refractory Materials used in Metal Production Technology” (CaRMa) is acknowledged. Technical support from Anne Støre and Jannicke Kvello, Sintef Industry, is also acknowledged.

References

1. Edwards, L., *The History and Future Challenges of Calcined Petroleum Coke Production and Use in Aluminum Smelting.* JOM, 2015. **67**(2): p. 308-321.

2. Edwards, L., et al., *Evolution of Anode Grade Coke Quality.* Light Metals, 2012: p. 1204-1212.
3. Houston, G.J. and H.A. Øye, *Consumption of anode carbon during aluminium electrolysis. I-III.* Aluminium, 1985. **61**: p. 251-254, 346-349, 426,428.
4. Xiao, J., et al., *Effect of sulfur impurity on coke reactivity and its mechanism.* Transactions of Nonferrous Metals Society of China, 2014. **24**(11): p. 3702-3709.
5. Bensah, Y.D. and T. Foosnaes, *The nature and effect of sulphur compounds on co 2 and air reactivity of petrol coke.* Journal of Engineering and Applied Sciences, 2010. **5**(6): p. 35-43.
6. Hume, S.M., et al., *Influence of Petroleum Coke Sulphur Content on the Sodium Sensitivity of Carbon Anodes.* Light Metals, 1993: p. 535-541.
7. Jahrsengene, G., et al., *A XANES Study of Sulfur Speciation and Reactivity in Cokes for Anodes Used in Aluminum Production.* Metallurgical and Materials Transactions B, 2018. **49**(3): p. 1434-1443.
8. Washburn, E.W., *Note on a Method of Determining the Distribution of Pore Sizes in a Porous Material.* Proceedings of the National Academy of Sciences of the United States of America, 1921. **7**(4): p. 115-116.
9. Brunauer, S., P.H. Emmett, and E. Teller, *Adsorption of Gases in Multimolecular Layers.* Journal of the American Chemical Society, 1938. **60**(2): p. 309-319.
10. Barrett, E.P., L.G. Joyner, and P.P. Halenda, *The Determination of Pore Volume and Area Distributions in Porous Substances. I. Computations from Nitrogen Isotherms.* Journal of the American Chemical Society, 1951. **73**(1): p. 373-380.
11. Olivier, J.P., *Chapter Seven - The Surface Heterogeneity of Carbon and Its Assessment A2 - Bottani, Eduardo J*, in *Adsorption by Carbons*, J.M.D. Tascón, Editor. 2008, Elsevier: Amsterdam. p. 147-166.
12. Olivier, J.P. and M. Winter, *Determination of the absolute and relative extents of basal plane surface area and "non-basal plane surface" area of graphites and their impact on anode performance in lithium ion batteries.* Journal of Power Sources, 2001. **97-98**: p. 151-155.
13. Thommes, M., et al., *Physisorption of gases, with special reference to the evaluation of surface area and pore size distribution (IUPAC Technical Report)*. Vol. 87. 2015.
14. Figueiredo, J.L., et al., *Modification of the surface chemistry of activated carbons.* Carbon, 1999. **37**(9): p. 1379-1389.
15. Tan, Z., *Chapter 2 - Basic Properties of Gases*, in *Air Pollution and Greenhouse Gases*. 2014.
16. Slattery, J.C. and R.B. Bird, *Calculation of the diffusion coefficient of dilute gases and of the self-diffusion coefficient of dense gases.* AIChE Journal, 1958. **4**(2): p. 137-142.